$CD34^{+}THY1^{+}$ Synovial Fibroblast Subset in Arthritic Joints Has High Osteoblastic and Chondrogenic Potentials in Vitro

Seiji Noda
Department of Rheumatology, Tokyo Medical and Dental University Graduate School of Medical and Dental Sciences: Tokyo Ika Shika Daigaku Daigakin Ishigaku Sogo Kenkyuka https://orcid.org/0000-0003-0268-8446

Tadashi Hosoya
Department of Rheumatology, Tokyo Medical and Dental University Faculty of Medicine: Tokyo Ika Shika Daigaku Daigakin Ishigaku Sogo Kenkyuka

Yoji Komiya
Department of Rheumatlogy, Tokyo Medical and Dental University Graduate School of Medical and Dental Sciences: Tokyo Ika Shika Daigaku Daigakin Ishigaku Sogo Kenkyuka

Yasuhiro Tagawa
Department of Rheumatology, Tokyo Medical and Dental University Graduate School of Medical and Dental Sciences: Tokyo Ika Shika Daigaku Daigakin Ishigaku Sogo Kenkyuka

Kentaro Endo
Center for Stem Cell and Regenerative Medicine, Tokyo Medical and Dental University Faculty of Medicine: Tokyo Ika Shika Daigaku Daigakin Ishigaku Sogo Kenkyuka

Keiichiro Komori
Center for Stem Cell and Regenerative Medicine, Tokyo Medical and Dental University Graduate School of Medical and Dental Sciences: Tokyo Ika Shika Daigaku Daigakin Ishigaku Sogo Kenkyuka

Hideyuki Koga
Department of Joint Surgery and Sports Medicine, Tokyo Metropolitan University Graduate School and Faculty of Science: Tokyo Toritsu Daigaku Rigakubu Daigakuin Rigaku Kenkyuka

Yasuhiro Takahara
Department of Orthopedics, Nippon Koukan Fukuyama Hospital

Kazutaka Sugimoto
Department of Orthopedics, Sonodakai joint Replacement Center Hospital

Ichiro Sekiya
Center for Stem Cell and Regenerative Medicine, Tokyo Medical and Dental University Faculty of Medicine: Tokyo Ika Shika Daigaku Daigakin Ishigaku Sogo Kenkyuka

Tetsuya Saito

Department of Rheumatology, Tokyo Medical and Dental University Graduate School of Medical and Dental Sciences: Tokyo Ika Shika Daigaku Daigakin Ishigaku Sogo Kenkyuka

Fumitaka Mizoguchi

Department of Rheumatology, Tokyo Medical and Dental University Graduate School of Medical and Dental Sciences: Tokyo Ika Shika Daigaku Daigakin Ishigaku Sogo Kenkyuka

Shinsuke Yasuda (syasuda.rheu@tmd.ac.jp)

Tokyo Medical and Dental University

Research article

Keywords: Synovial fibroblasts, osteogenic, enhancement, rheumatoid arthritis

Posted Date: October 28th, 2021

DOI: https://doi.org/10.21203/rs.3.rs-1006154/v1

Version of Record: A version of this preprint was published at Arthritis Research & Therapy on February 15th, 2022. See the published version at https://doi.org/10.1186/s13075-022-02736-7.

Abstract

Objective: Synovial fibroblasts (SF)s in rheumatoid arthritis (RA) and osteoarthritis (OA) play biphasic roles in joint destruction and regeneration of bone/cartilage as mesenchymal stem cells (MSC)s. Although MSCs contribute to joint homeostasis, such function is impaired in arthritic joints. We have identified functionally distinct three SF subsets characterized by the expression of CD34 and THY1 as follows: $CD34^{+}THY1^{+}$, $CD34^{-}THY1^{-}$ and $CD34^{-}THY1^{+}$. The objective of this study was to clarify the differentiation potentials as MSCs in each SF subset since both molecules would be associated with the MSC function.

Methods: SF subsets were isolated from synovial tissues of 70 patients (RA: 18, OA: 52). Expressions of surface markers associated with MSCs (THY1, CD73, CD271, CD54, CD44 and CD29) were evaluated in fleshly-isolated SF subsets by flow cytometry. The differentiation potentials of osteogenesis, chondrogenesis, and adipogenesis were evaluated with histological staining and quantitative polymerase chain reaction of differentiation marker genes. Small interfering RNA was examined to deplete THY1 in SFs.

Results: The expression levels of $THY1^{+}$, $CD73^{+}$ and $CD271^{+}$ were highest and those of $CD54^{+}$ and $CD29^{+}$ were lowest in $CD34^{+}THY1^{+}$ among three subsets. Comparing three subsets, the calcified area, alkaline phosphatase (ALP)-stained area and cartilage matrix subset were the largest in $CD34^{+}THY1^{+}$ subset. Consistently, the expressions of differentiation markers of the osteoblasts (*RUNX2, ALPL* and *OCN*) or chondrocytes (*ACAN*) were the highest in $CD34^{+}THY1^{+}$ subset, indicating that $CD34^{+}THY1^{+}$ subset possessed the highest osteogenic and chondrogenic potential among three subsets. While the differentiation potentials to adipocytes were comparable among the subsets regarding lipid droplet formations and the expression of *LPL* and *PPARγ*. The knockdown of THY1 in bulk SFs resulted in impaired osteoblast differentiation indicating some functional aspects in this stem-cell marker.

Conclusion: $CD34^{+}THY1^{+}$ SF subset has high osteogenic and chondrogenic potentials. The preferential enhancement of MSCs functions in $CD34^{+}THY1^{+}$ subset may provide a new treatment strategy for regenerating damaged bone/cartilage in arthritic joints.

Background

In rheumatoid arthritis (RA) and osteoarthritis (OA), the joint function is impaired due to cartilage and bone damage. The affected patients suffered from the decline of physical status, resulting in a shortening in healthy life expectancy (1). The homeostatic responses of the joint environments, including the joint repairing, were impaired because of chronic inflammation and mechanical stress (2). According to these clinical situations, the strategy to enhance tissue regeneration would be a possible strategy to construct complementary treatment.

Synovial fibroblasts (SF)s are contributing to the pathogenesis of RA and OA by secreting inflammatory cytokines, tissue degrading factors, and making pannus formation (2–3). SFs also possess several characteristics of mesenchymal stem cells (MSC)s, including self-renewal capacity and multi-lineage differentiation potentials to mesenchymal tissues (4–5). MSCs isolated from synovial tissue can be more efficiently differentiated into chondrocytes than those from other tissue (e.g. bone marrow) (6–7). In addition, MSCs are proliferated in response to mechanical stress or inflammatory cytokines (8–9), suggesting that they can be induced under disease conditions in RA and OA. Since MSC functions as osteogenesis and chondrogenesis were induced in case of bone damages or bone fractures (10–12), the therapeutic application of synovial MSCs would have a potent for the repairment of bone erosion in RA.

We previously reported that SFs in arthritic joints are composed of three functionally distinct subsets, $CD34^{-}THY1^{-}$, $CD34^{-}THY1^{+}$ and $CD34^{+}THY1^{+}$ population based on the expression of CD34 and THY1 (13). $CD34^{-}THY1^{+}$ subset was found to be expanded in patients with RA, whereas the proportion of $CD34^{+}THY1^{+}$ subset was comparable between RA and OA. Both subsets possessed pathological functions, including proinflammatory cytokines secretions, high proliferation capacity, and enhanced invasiveness when compared with $CD34^{-}THY1^{-}$ subset. THY1 and CD34 are the MSCs surface markers related to wound repair as well as lineage potentials in osteogenesis and chondrogenesis (14–15). Since we and others have already elucidated that the functions of $THY1^{-}/THY1^{+}$ SF are distinct (16–18), we hypothesized that three SF subsets have a different function as MSC, and that baseline expression of THY1 in SF subsets would determine the differentiation potentials. Indeed, $THY1^{+}CD73^{+}$ SF subset presented higher chondrogenic potentials than $THY1^{-}CD73^{+}$ subset (19).

In the present study, we evaluated the MSCs function of each SF subset regarding differentiation potential to osteoblast, chondrocyte, and adipocyte. Here we demonstrate that $CD34^{+}THY1^{+}$ subset have MSC potential than the others regardless of the background diseases, suggesting future therapeutic applications utilizing MSC function in this subset.

Methods

Patient recruitment and isolation of synovial cells

We obtained synovial tissues from surgeries of joint replacement for patients with OA and RA. We consecutively collected all the available OA and RA samples for this study. Written informed consent for this study and the ethics approval from medical research ethics committee of Tokyo Medical and Dental University (Approval number: M2000-979) were obtained. The synovial tissues were collected from 70 patients (RA:18, OA: 52). All the patients with RA have been received treatment with disease modified anti-rheumatic drugs (DMARD)s including biologics. Ten patients were administered steroids (average dose; 2.9 mg/day). Other characteristics are described in Table 1.

Tissue samples were collected consecutively from joint replacement surgeries to eliminate any bias as previously reported (13). Briefly, joint tissues were obtained immediately after the surgeries, followed by

removal of bone and adipose tissues with scissors. Synovial tissues were minced into small pieces, and then subjected to enzymatic digestion. For cell culture, we digested tissues with 2 mg/mL collagenase type 4 (Worthington, NJ, USA), 0.8 mg/mL Dispase II, 0.1 mg/mL DNase I (Roche, Basel, Switzerland) in Dulbecco's modified Eagle Roche's medium (DMEM) at 37 °C. After 15 min, we collected the supernatant and replaced with fresh enzyme mix. These procedures were repeated every 15 min for total 1 h. After lysing red blood cells with ACK-lysing buffer, obtained cells were treated with antibodies as described below then sorted by FACS Aria II and III (BD Biosciences, CA, USA) with 100 μm nozzle.

Antibodies

The following antibodies and reagents were used for the analysis of synovial cells with flow cytometry and cell sorting: anti-CD45-APC-H7 (2D1, BD Biosciences, CA, USA), anti-CD235a-APC-Alexa Fluor750 (11E4B-7-6, Beckman Coulter, FL, USA), anti-CD31-PE-Cyanine7 (WM-59, eBioscience, CA, USA), anti-CD146-APC (P1H12, eBioscience), anti-CD34-PE (4H11, eBioscience), anti-PDPN-PerCP-eFluor710 (NZ-1.3, eBioscience), anti-THY1-FITC (5E10, BD Bioscience), anti-CD73-PE-CF594 (AD2, BD Bioscience), anti-CD271-APC (ME20.4, eBioscience), anti-CD54-PE-CF594 (HA58 BioLegend, CA, USA), anti-CD44-APC (G44-26 BD Bioscience), anti-CD29-APC (TS2/16 BioLegend), human TruStain FcX (BioLegend) and Live/Dead fixable aqua dead cell stain kits (Molecular Probes, Thermo Fisher Scientific, MA, USA).

Flow cytometry analysis

The gating strategy of SF subsets was as shown (Supplementary Figure 1). While the mean ratios of $CD34^{-}THY1^{-}$, $CD34^{-}THY1^{+}$ and $CD34^{+}THY1^{+}$ subsets in RA were 35.5%, 24.1% and 24.8%, respectively, the mean ratios of these subsets in OA were 56.6%, 10.2% and 17.2%. These results were compatible as previously reported (13).

We evaluated the expression of MSC surface markers (THY1, CD73, CD271, CD54, CD29 and CD44) in the SF subsets. Considering the expression of MSC markers in the freshly-isolated synovial cells, we evaluated the mean fluorescence intensity (MFI) as expression levels of these markers in the individual subsets by flow cytometry in the 12 consecutive samples (RA: 3, OA: 9) (Supplementary Figure 2).

Cell culture

We sorted $CD34^{-}THY1^{-}$ fibroblasts, $CD34^{-}THY1^{+}$ fibroblasts and $CD34^{+}THY1^{+}$ fibroblasts and cultured them in DMEM supplemented with 10% FBS (Gemini Bio, CA, USA), 2 mM L-glutamine, antibiotics (penicillin and streptomycin), and essential and nonessential amino acids (Life Technologies, CA, USA). The cells were expanded for 20-30 days for assays.

Osteoblast, chondrogenic and adipocyte differentiation

Osteoblastic induction was performed as previously reported (6). 3.0×10^3 cells/cm^2 were plated in a 12-well plate in osteogenic differentiation medium containing L-ascorbic acid-2-phosphate (0.2 mM; Wako Pure Chemical Industries, Osaka, Japan), beta-glycerophosphate (5 mM; Wako Pure Chemical Industries),

dexamethasone (1 nM; Wako Pure Chemical Industries) and incubated at 37 °C in 5 % CO_2. All media were changed twice per week. Each SF subset was cultured for 3-4 weeks. Histological staining was performed with alizarin red (Merk Millipore, MA, USA) and alkaline phosphatase (ALP) staining for osteoblast differentiation

For chondrogenic differentiation, 1.25-2.5 × 10^5 cells were placed in a 15-mL polypropylene tube (AGC Techno Glass Co., Ltd, Shizuoka, Japan) and centrifuged at 1,500 × g for 5 min. The cells were cultured in chondrogenic induction medium containing 1,000 ng/mL of BMP-2 (PeproTech, NJ, USA) and 10 ng/mL of transforming growth factor-β3 (PeproTech), incubated at 37 °C in 5% CO_2 for 3 weeks. All media were changed twice per week. Histological staining was performed with safranin O staining for chondrogenesis.

For Adipogenesis, 7.0 × 10^3 cells/cm^2 are plated and cultured in StemPro™ Adipogenesis Differentiation Kit (Gibco, Thermo Fisher Scientific, MA, USA) for 3 weeks. All media were changed twice per week. Oil-red staining was used to evaluate adipogenesis.

For chondrogenesis and adipocyte differentiation, we referred to the previous reports with some modifications (20-21). Briefly, we performed some pellet culture at a density of 1.25 × 10^5 cells due to imbalance in the number of each subset.

Quantitative real-time Polymerase chain reaction (qPCR)

cDNA was synthesized with QuantiTect Reverse Transcription kit (Qiagen, Hilden, German). Quantitative polymerase chain reaction (qPCR) was performed with Brilliant III Ultra-Fast SYBR Green qPCR master mix (Agilent Technologies, CA, USA) on a LightCycler96® (Roche). The following primers were used as shown in Table 2.

Knockdown of gene expression by small interfering (si) RNA

SFs were seeded at 1.2 × 10^4 into 12-well cell culture plates and subsequently transiently transfected with 20 pM of THY1 or control small interfering (si) RNA (Thermo Fisher Scientific) using Lipofectamine RNAiMax (Thermo Fisher Scientific) according to the manufacturer's protocol. Cells were incubated with siRNA for 3 day and subjected to osteogenic differentiation as described above.

Results

$CD34^+THY1^+$ subset expressed MSC surface markers

Considering the expression of surface markers in the freshly-isolated synovial cells, both $CD34^+THY1^+$ and $CD34^-THY1^+$ subsets expressed THY1 with higher levels than $CD34^-THY1^-$ subset, as we have shown previously (13). Interestingly, the expression level of THY1 in $CD34^+THY1^+$ was the highest among the SF subsets regardless of the underlying diseases (Figure 1A).

The expressions of CD73 and CD271 were the highest in $CD34^+THY1^+$ subset among three subsets (Figure 1B), whereas the expression levels of CD54 and CD29, a surface marker with low osteogenic potentials in derived from other cell types (22-23), was lower in $CD34^+THY1^+$ subset than $CD34^-THY1^-$ subset (Figure 1B). The expression level of CD44 was not significantly different among three subsets (Figure 1B).

Regarding the transcriptions of MSC surface markers in microarray data, theses were not significant difference among three subsets (Supplementary Figure 3), indicating that these molecules are not regulated differently at the transcriptional levels.

$CD34^+$ $THY1^+$ subset presented the highest osteogenic potentials.

The average ratio of calcified area stained with alizarin red as red spots was 4- and 1.5- times higher in $CD34^+THY1^+$ subsets than $CD34^-THY1^-$ and $CD34^-THY1^+$ subsets (Figure 2A and 2B). We also stained three SF subsets with ALP staining to verify whether observed calcification is due to the differentiation of $CD34^+THY1^+$ SFs into osteoblasts. The activity of ALP, which was expressed as blue stained area, was observed at twice higher levels in $CD34^+$ $THY1^+$ subset (Figure 2A and 2B) than $CD34^-THY1^-$ subset.

To confirm the osteoblast differentiation by quantifying differentiation associated genes, the expressions of mRNA levels were measured. The expression levels of *RUNX2*, master regulator for osteoblast differentiation (24), was 2.8-times higher in $CD34^+THY1^+$ subset than $CD34^-THY1^-$ subset (Figure 2C). As for expression levels of *ALPL,* which is a marker in the early stage of osteoblast differentiation was expressed 1.8-times higher in $CD34^+THY1^+$ subset than other two subsets after the differentiation for 3 weeks (Figure 2C). The expression levels of *OCN*, a differentiation marker in the mature osteoblast, were 1.7-times higher in $CD34^+THY1^+$ subset than $CD34^-THY1^-$ subset after the differentiation for 4 weeks (Figure 2C). These findings indicate that $THY1^+$ subsets, especially $CD34^+THY1^+$ subset is the subset with the most superior osteogenic potentials in vitro.

$CD34^+$ $THY1^+$ subset possessed the highest chondrocyte differentiation potentials.

After the culture in chondrogenic differentiation medium for 3 weeks, the largest chondrocyte pellets were formed from $CD34^+THY1^+$ subset (Figure 3A). The ratio of cartilage matrix stained as red by Safranin-O staining in $CD34^-THY1^-$, $CD34^-THY1^+$ and $CD34^+THY1^+$ subsets were 39%, 41% and 46%, respectively (Figure 3B). $CD34^+THY1^+$ subset presented significantly higher ratio of cartilage matrix than $CD34^-THY1^-$ subsets.

Confirming the quantitative verification of chondrogenesis, expression levels of *ACAN*, which codes aggrecan, were evaluated. In both $CD34^-THY1^+$, and $CD34^+THY1^+$ subsets, *ACAN* expression levels were 2.8- and 8- times higher than in $CD34^-$ $THY1^-$ subset, respectively (Figure 3B). These findings indicated that $THY1^+$ subsets, especially $CD34^+THY1^+$ subset has the highest chondrogenic potential in vitro.

Adipocyte differentiation potential was not significantly different among the subsets.

After culture in the adipocyte differentiation medium for 3 weeks, all SF subsets comparably presented lipid droplets (Figure 4A). The expressions of adipocyte associated genes, including *LPL* and *PPARγ*, which codes lipoprotein lipase and peroxisome proliferator-activated receptor γ, were evaluated. The expression levels of *LPL* and *PPARγ* transcripts were not significantly different (Figure 4B).

These findings indicated that osteogenic and chondrogenic potentials were relatively high in $CD34^{+}THY1^{+}$ subset, whereas adipogenic potential was comparable among three subsets.

THY1 knockdown suppressed osteoblast differentiation

Since THY1 is one of the MSCs surface marker and associated with lineage potentials in osteogenesis and chondrogenesis, we hypothesized that baseline expression of THY1 in SF subsets determined differentiation potentials. Therefore, we investigated the endogenous function of THY1 in the osteoblast differentiation by the depletion using RNA-interference.

Compared with those treated with siRNA control, THY1 deficient SF demonstrated impaired calcification as well as attenuated ALP activity after 4 weeks culture in osteogenic differentiation medium (Figure 5A and 5B). Expressions of *THY1*, *RUNX2* and *ALPL* were also significantly suppressed (Figure 5C). These findings supported the hypothesis that the expression of endogenous THY1 is inevitable for the MSC functions in $CD34^{+}THY1^{+}$ subset.

Discussion

In the present study we identified significantly higher differentiation potency in $CD34^{+}THY1^{+}$ subset by evaluating the osteogenic and chondrogenic differentiation potentials. The pattern of the MSC-associated surface markers also supported the highest potential as MSCs in $CD34^{+}THY1^{+}$ subset.

Our findings were consistent with the previous reports that THY1 expression was associated with osteogenesis in bone marrow-derived MSCs (25). Additionally, THY1 is involved in angiogenesis through the differentiation of endothelial cells (26). In arthritic joints, perivascular SFs are exposed to Notch3 signaling from vascular endothelial cells, which is essential in the induction and maintenance of the expression of THY1 (27). $THY1^{+}$ subsets, which predominantly localize at the perivascular lesion in the synovium, may be induced due to angiogenesis followed by synovitis and joint damage. In contrast to the differentiation potentials, THY1 interacts with integrin and induces cell apoptosis via activation of caspase 3/7 pathway (28–29). Since THY1 expression was enhanced in fibroblasts when joint tissue was injured (30–31), these findings suggest that THY1 exerts to orchestrate the maintenance of joint homeostasis. In the arthritic joints, $CD34^{+}THY1^{+}$ subset might be induced compensatory by the mechanical stress/injury in the joints.

In addition to THY1, we identified CD34 as a complementary marker to enrich MSCs from freshly-isolated synovial cells. Since CD34, a marker for hematopoietic stem cells (32), was used as a negative marker for MSC isolation so far, CD34 is positive in freshly isolated bone marrow-derived MSC (BMSC)s and $CD34^+$ BMSCs produced greater fibroblast colony-forming units than $CD34^-$ BMSCs (33). CD34 is also expressed not only on hematopoietic stem cells but also 10% of circulating fibrocytes, which are recruited to the injured site and associated with inflammation and wound repair (34–36). Although the potentials to differentiate osteoblasts and chondrocytes circulating fibrocytes have been analyzed in fibrotic lung tissue (37), the differentiation potentials in SFs, especially $CD34^{+/-}$ populations have not been compared. Therefore, this is the first report evaluating the MSC function in $CD34^+THY1^+$ double-positive SF subset.

In active arthritis, the osteogenic and chondrogenic differentiation potentials in $THY1^+$ subsets may be overwhelmed or impaired due to inflammation. Although TNF and IL-6 blocking therapy have similar efficacy for RA patients (38), erosion repairment was observed most frequently under treatment with IL-6 blocking therapy (39–40). Since MSC functions were enhanced in the presence of inflammatory cytokines, including IL-1β or TNF α (8)(41), bone repair would result from the fine-tuning of inflammatory mediators in the arthritic joint. Suppression of several inflammatory cytokines ameliorate arthritis effectively, whereas these might not be beneficial for inducing MSC functions.

As $CD34^+THY1^+$ subset has a highly potent MSC function, these cell population might be appropriate to be applied for joint repairing therapy. However, $CD34^+THY1^+$ subset would simultaneously contribute to the RA pathogenesis by the secretion of inflammatory cytokines and by enhanced proliferation potential (13). We need to find the way to preferentially utilize the MSC function in $THY1^+$ subsets or modify pro-inflammatory cytokine production in $CD34^+THY1^+$ for the further therapeutic application. To enhance MSC potentials, we would consider several approaches to induce the expression of $THY1^+$ in SFs. Jagged 1 and Delta-like 4, which are one of the Notch3 ligands, may be useful for THY1 induction (27)(42). Stimulation of Notch3 signaling may be applicable to acquire osteogenic and chondrogenic differentiation potentials in SFs. A low oxygen environment is beneficial for MSC expansion and chondrogenesis by activating hypoxia-inducible factor α and upregulation of THY1 (43).

Direct introduction of MSCs in the inflammatory joints has been proved to have immunosuppressive effects by induction of inducible regulatory T cells, which leads to inhibition of T cell proliferation and cytokine production (44). In addition, their systemic administration improves arthritis by inhibiting osteoclasts differentiation in arthritic animal model (45). Clinical trials by administrating human MSCs into joint spaces have been examined (4)(46–47). Alternatively, MSCs-derived exosomes, but not MSCs themselves, would be candidates for a novel treatment strategy for RA and OA since they can promote chondrogenesis (48).

Our study comprises several limitations. First, more than half of the synovial tissues were derived from OA, and the comparison of differentiation potential between RA and OA was not sufficient. Second, osteogenic and chondrogenic potentials in $CD34^+THY1^+$ subset were not evaluated under the *in vivo*

environment. Third, we had not analyzed the relevance of previously reported signaling pathways, including Wnt pathway (49).

Conclusions

The multipotency of differentiation in SFs has drawn attention of researchers as such MSC-like characteristics would expect us to develop novel therapeutic strategies for joint repair in RA and/or OA. $CD34^{+}THY1^{+}$ subset presented high osteogenic and chondrogenic differentiation potentials. This subset also most intensively expressed MSC positive surface markers at the protein level, CD73 and CD271 as well as THY1. The preferential enhancement of MSCs functions in $CD34^{+}THY1^{+}$ subset may provide a new treatment strategy in regeneration of damaged bone/cartilage in advanced RA and/or OA.

Abbreviations

synovial fibroblast: SF

rheumatoid arthritis: RA

osteoarthritis: OA

mesenchymal stem cells: MSCs

biologic/conventional disease modified anti-rheumatic drug: b/c DMARD

mean fluorescence intensity: MFI

quantitative polymerase chain reaction: qPCR

interleukin: IL

tumor necrosis factor: TNF

methotrexate: MTX

alkaline phosphatase: ALP

osteocalcin: OCN

aggrecan: ACAN

lipoprotein lipase: LPL

peroxisome proliferator-activated receptor γ: PPARγ

small interfering RNA: siRNA

Declarations

Ethics approval and consent to participate

Written informed consent for publication was obtained from all the patients.

We have confirmed the ethics approval from medical research ethics committee of Tokyo Medical and Dental University (Approval number: M2000-979).

Consent for publication

We have obtained written informed consent for publication from all the patients.

Availability of data and materials

The datasets generated during and analysed during the current study are available from the corresponding author on reasonable request.

The microarray data used in the current study is available in https://www.ncbi.nlm.nih.gov/geo/geo2r/?acc=GSE109450&platform=GPL18573.

Competing interests

The authors declare that there is no conflict of interest.

Funding

This work was supported by Grant-in-Aid for Scientific Research (C) Grant Number JP19K08903, Grant-in-Aid for Early-Career Scientists Grant Number JP19K17884, Health Labour Sciences Research Grant Number 2309302-1, Japan Reserch Foundation Clinical Pharmacology Grant Number 91AA003257, AMED under Grant Number AA400139 and donation from Bristol Myers Squibb, Mitsubishi Tanabe Pharma, Takeda Pharmaceutical Company Limited, Sanofi, Novartis Pharma and Abbvie.

Authors' contributions

SN, IS, SY and FM designated the research. SN, KE and YK performed all the examination. SN, TH, FM and SY analyzed and interpreted data.SN drafted the manuscript. TH, YK, YT, KE, KK, HK, YT, KS, IS, TS and SY supervised the manuscript. The final manuscript has been approved for publication by all the authors.

Acknowledgements

The authors thank Assistant Professor Yukie Tanaka for the technical support of FACS analysis in this study.

References

1. Reynolds SL, McIlvane JM. The impact of obesity and arthritis on active life expectancy in older Americans. Obesity. 2009;17:363–9.
2. Boissier MC, Semerano L, Challal S, Saidenberg-Kermanac'h N, Falgarone G. Rheumatoid arthritis: From autoimmunity to synovitis and joint destruction. J Autoimmun. 2012;39:222–8.
3. Scanzello CR, Goldring SR. The role of synovitis in osteoarthritis pathogenesis. Bone. 2012;51:249–57.
4. Oreffo ROC, Cooper C, Mason C, Clements M. Mesenchymal stem cells lineage, plasticity, and skeletal therapeutic potential. Stem Cell Rev. 2005;1:169–78.
5. Dominici M, Le Blanc K, Mueller I, Slaper-Cortenbach I, Marini FC, Krause DS, et al. Minimal criteria for defining multipotent mesenchymal stromal cells. The International Society for Cellular Therapy position statement. Cytotherapy. 2006;8:315–7.
6. De Bari C, Dell'Accio F, Tylzanowski P, Luyten FP. Multipotent mesenchymal stem cells from adult human synovial membrane. Arthritis Rheum. 2001;44:1928–42.
7. Yoshimura H, Muneta T, Nimura A, Yokoyama A, Koga H, Sekiya I. Comparison of rat mesenchymal stem cells derived from bone marrow, synovium, periosteum, adipose tissue, and muscle. Cell Tissue Res. 2007;327:449–62.
8. Matsumura E, Tsuji K, Komori K, Koga H, Sekiya I, Muneta T. Pretreatment with IL-1β enhances proliferation and chondrogenic potential of synovium-derived mesenchymal stem cells. Cytotherapy. 2017;19:181–93.
9. Yen KL, Capilla E, Rosen CJ, Gilsanz V, Pessin JE, Judex S, et al. Mechanical stimulation of mesenchymal stem cell proliferation and differentiation promotes osteogenesis while preventing dietary-induced obesity. J Bone Miner Res. 2009;24:50–61.
10. Su P, Tian Y, Yang C, Ma X, Wang X, Pei J, et al. Mesenchymal stem cell migration during bone formation and bone diseases therapy. Int J Mol Sci. 2018;19.
11. Giuliani N, Lisignoli G, Magnani M, Racano C, Bolzoni M, Dalla Palma B, et al. New insights into osteogenic and chondrogenic differentiation of human bone marrow mesenchymal stem cells and their potential clinical applications for bone regeneration in pediatric orthopaedics. Stem Cells Int. 2013;2013.
12. Sekiya I, Katano H, Ozeki N. Characteristics of mscs in synovial fluid and mode of action of intra-articular injections of synovial mscs in knee osteoarthritis. Int J Mol Sci. 2021;22:1–13.
13. Mizoguchi F, Slowikowski K, Wei K, Marshall JL, Rao DA, Chang SK, et al. Functionally distinct disease-associated fibroblast subsets in rheumatoid arthritis. Nat Commun. 2018;9:1–11.
14. Scott S, Clouser C, Aho J. Methods to Validate Mesenchymal Stem Cell Quality. Bio-Techne. 2015;5–6.
15. Rege TA, Hagood JS. Thy-1 as a regulator of cell-cell and cell-matrix interactions in axon regeneration, apoptosis, adhesion, migration, cancer, and fibrosis. FASEB J. 2006;20:1045–54.

16. Zhang F, Wei K, Slowikowski K, Fonseka CY, Rao DA, Kelly S, et al. Defining inflammatory cell states in rheumatoid arthritis joint synovial tissues by integrating single-cell transcriptomics and mass cytometry. Nat Immunol. 2019;20:928–42.
17. Croft AP, Campos J, Jansen K, Turner JD, Marshall J, Attar M, et al. Distinct fibroblast subsets drive inflammation and damage in arthritis. Nature. 2019;570:246–51.
18. Alivernini S, MacDonald L, Elmesmari A, Finlay S, Tolusso B, Gigante MR, et al. Distinct synovial tissue macrophage subsets regulate inflammation and remission in rheumatoid arthritis. Nat Med. 2020;26:1295–306.
19. Sivasubramaniyan K, Koevoet WJLM, Hakimiyan AA, Sande M, Farrell E, Hoogduijn MJ, et al. Cell-surface markers identify tissue resident multipotential stem / stromal cell subsets in synovial intimal and sub-intimal compartments with distinct chondrogenic properties. Osteoarthr Cartil. 2019;27:1831–40.
20. Mizuno M, Katano H, Mabuchi Y, Ogata Y, Ichinose S, Fujii S, et al. Specific markers and properties of synovial mesenchymal stem cells in the surface, stromal, and perivascular regions. Stem Cell Res Ther. 2018;9:1–11.
21. Chang Q, Li C, Lu Y, Geng R, Wei J nan, Hu J zheng. Adipose-derived mesenchymal stromal cells suppress osteoclastogenesis and bone erosion in collagen-induced arthritis. Scand J Immunol. 2020;92:135–44.
22. Zhao L, Abdollah P, Do S, Nye C, Hantash BM. Novel Negative Selection Marker CD54 Enhances Differentiation of Human Adipose-Derived Mesenchymal Stem Cells. Immunol, J Clin Cell. 2013;S9.
23. Suto EG, Mabuchi Y, Suzuki N, Suzuki K, Ogata Y, Taguchi M, et al. Prospectively isolated mesenchymal stem/stromal cells are enriched in the CD73+ population and exhibit efficacy after transplantation. Sci Rep. 2017;7:1–10.
24. Thiagarajan L, Abu-Awwad HADM, Dixon JE. Osteogenic Programming of Human Mesenchymal Stem Cells with Highly Efficient Intracellular Delivery of RUNX2. Stem Cells Transl Med. 2017;6:2146–59.
25. Picke AK, Campbell GM, Blüher M, Krügel U, Schmidt FN, Tsourdi E, et al. Thy-1 (CD90) promotes bone formation and protects against obesity. Sci Transl Med. 2018;10.
26. Schubert K, Gutknecht D, Köberle M, Anderegg U, Saalbach A. Melanoma cells use thy-1 (CD90) on endothelial cells for metastasis formation. Am J Pathol. 2013;182:266–76.
27. Wei K, Korsunsky I, Marshall JL, Gao A, Watts GFM, Major T, et al. Notch signalling drives synovial fibroblast identity and arthritis pathology. Nature. 2020;582:259–64.
28. Schmidt M, Gutknecht D, Anastassiadis K, Eckes B, Anderegg U, Saalbach A. Thy-1/β3 Integrin Interaction-Induced Apoptosis of Dermal Fibroblasts Is Mediated by Up-Regulation of FasL Expression. J Invest Dermatol. 2016;136:526–9.
29. Yang J, Zhan XZ, Malola J, Li ZY, Pawar JS, Zhang HT, et al. The multiple roles of Thy-1 in cell differentiation and regeneration. Differentiation. 2020;113:38–48.

30. Woeller CF, Flores E, Pollock SJ, Phipps RP. Thy1 (CD90) expression is reduced by the environmental chemical tetrabromobisphenol-A to promote adipogenesis through induction of microRNA-103. Toxicol Sci. 2017;157:305–19.
31. Saalbach A, Anderegg U, Bruns M, Schnabel E, Herrmann K, Haustein UF. Novel fibroblast-specific monoclonal antibodies: Properties and specificities. J Invest Dermatol. 1996;106:1314–9.
32. Colter David, Class Reiner DCMPDJ. Rapid expansion of recycling stem cells in cultures of plastic-adherent cells from human bone marrow. Proc Natl Acad Sci U S A. 2000;97:3213–8.
33. Simmons PJ, Torok-Storb B. CD34 expression by stromal precursors in normal human adult bone marrow. Blood. 1991;78:2848–53.
34. Strieter RM, Keeley EC, Hughes MA, Burdick MD, Mehrad B. The role of circulating mesenchymal progenitor cells (fibrocytes) in the pathogenesis of pulmonary fibrosis. J Leukoc Biol. 2009;86:1111–8.
35. Bucala R. Circulating Fibrocytes: Cellular Basis for NSF. J Am Coll Radiol. 2008;5:36–9.
36. Sidney LE, Branch MJ, Dunphy SE, Dua HS, Hopkinson A. Concise review: Evidence for CD34 as a common marker for diverse progenitors. Stem Cells. 2014;32:1380–9.
37. Choi YH, Burdick MD, Strieter RM. Human circulating fibrocytes have the capacity to differentiate osteoblasts and chondrocytes. Int J Biochem Cell Biol. 2010;42:662–71.
38. Lauper K, Mongin D, Iannone F, Kristianslund EK, Kvien TK, Nordström DC, et al. Comparative effectiveness of TNF inhibitors and tocilizumab with and without conventional synthetic disease-modifying antirheumatic drugs in a pan-European observational cohort of bio-naïve patients with rheumatoid arthritis. Semin Arthritis Rheum. 2020;50:17–24.
39. Finzel S, Rech J, Schmidt S, Engelke K, Englbrecht M, Schett G. Interleukin-6 receptor blockade induces limited repair of bone erosions in rheumatoid arthritis: A micro CT study. Ann Rheum Dis. 2013;72:396–400.
40. Finzel S, Kraus S, Figueiredo CP, Regensburger A, Kocijan R, Rech J, et al. Comparison of the effects of tocilizumab monotherapy and adalimumab in combination with methotrexate on bone erosion repair in rheumatoid arthritis. Ann Rheum Dis. 2019;78:1186–91.
41. Shioda M, Muneta T, Tsuji K, Mizuno M, Komori K, Koga H, et al. TNFα promotes proliferation of human synovial MSCs while maintaining chondrogenic potential. PLoS One. 2017;12:1–15.
42. Pagie S, Gérard N, Charreau B. Notch signaling triggered via the ligand DLL4 impedes M2 macrophage differentiation and promotes their apoptosis. Cell Commun Signal. 2018;16:1–12.
43. Pattappa G, Johnstone B, Zellner J, Docheva D, Angele P. The importance of physioxia in mesenchymal stem cell chondrogenesis and the mechanisms controlling its response. Int J Mol Sci. 2019;20:1–28.
44. González MA, González-Rey E, Rico L, Büscher D, Delgado M. Treatment of experimental arthritis by inducing immune tolerance with human adipose-derived mesenchymal stem cells. Arthritis Rheum. 2009;60:1006–19.

45. Oshita K, Yamaoka K, Udagawa N, Fukuyo S, Sonomoto K, Maeshima K, et al. Human mesenchymal stem cells inhibit osteoclastogenesis through osteoprotegerin production. Arthritis Rheum. 2011;63:1658–67.
46. Hyodo A, Ozeki N, Kohno Y, Suzuki S, Mizuno M, Otabe K, et al. Projected cartilage area ratio determined by 3-dimensional MRI analysis: Validation of a novel technique to evaluate articular cartilage. JBJS Open Access. 2019;4.
47. Aoki H, Ozeki N, Katano H, Hyodo A, Miura Y, Matsuda J, et al. Relationship between medial meniscus extrusion and cartilage measurements in the knee by fully automatic three-dimensional MRI analysis. BMC Musculoskelet Disord. 2020;21:1–9.
48. Mao G, Zhang Z, Hu S, Zhang Z, Chang Z, Huang Z, et al. Exosomes derived from miR-92a-3poverexpressing human mesenchymal stem cells enhance chondrogenesis and suppress cartilage degradation via targeting WNT5A. Stem Cell Res Ther. 2018;9:1–13.
49. Tang N, Song WX, Luo J, Luo X, Chen J, Sharff KA, et al. BMP-9-induced osteogenic differentiation of mesenchymal progenitors requires functional canonical Wnt/β-catenin signalling. J Cell Mol Med. 2009;13:2448–64.

Tables

Table 1: Patient characteristics.

	RA	OA
Number of patients	18	52
Treatment	bDMARDs:7	ND
	cDMARDs:14	ND
	(MTX:10, others:6)	ND
Average dose of prednisolone (mg/day)	2.9 (1-10)	ND
Average C reactive protein (mg/dL)	1.20 (0.02-6.04)	ND
Proportion of SF subsets		
$CD34^{-}THY1^{-}$	35.5% (8.1-83.2)	56.6% (22.1-87.1)
$CD34^{-}THY1^{+}$	24.1% (1.6-64.2)	10.2% (1.0-30.9)
$CD34^{+}THY1^{+}$	24.8% (2.1-55.7)	17.2% (0.8-56.9)

bDMARDs: biologic disease modified anti-rheumatic drugs

cDMARDs: conventional disease modified anti-rheumatic drugs

MTX: methotrexate

Table 2: Primers sequences used in the study.

Primer	Forward	Reverse
ALPL	5'ATGCTGAGTGACACAGACAAGAAG	5'GGTAGTTGTTGTGAGCATAGTCCAC
RUNX2	5’CATCACCGATGTGCCTAGG	5’TAAGTAAAGGTGGCTGGATAGTG
OCN	5’ GACTGTGACGAGTTGGCTG	5’ GGGAAGAGGAAAGAAGGGTG
ACAN	5’ TGTGGGACTGAAGTTCTTGG	5’AGCGAGTTGTCATGGTCTG
LPL	5’ACACTTGCCACCTCATTCC	5’ ACCCAACTCTCATACATTCCTG
PPARγ	5’GTCGGTTTCAGAAATCGGTTG	5’ GCTGGTCGATATCACTGGAG
THY1	5’ CTACTTATCCGCCTTCACTAGC	5’ TGATGCCCTCACACTTGAC
18S	5'ACTCAACACGGGAAACCTCA	5'AACCAGACAAATCGCTCCAC

ALPL: alkaline phosphatase, OCN: osteocalcin, ACAN: aggrecan, LPL: lipoprotein lipase, PPARγ: peroxisome proliferator-activated receptor γ

Figures

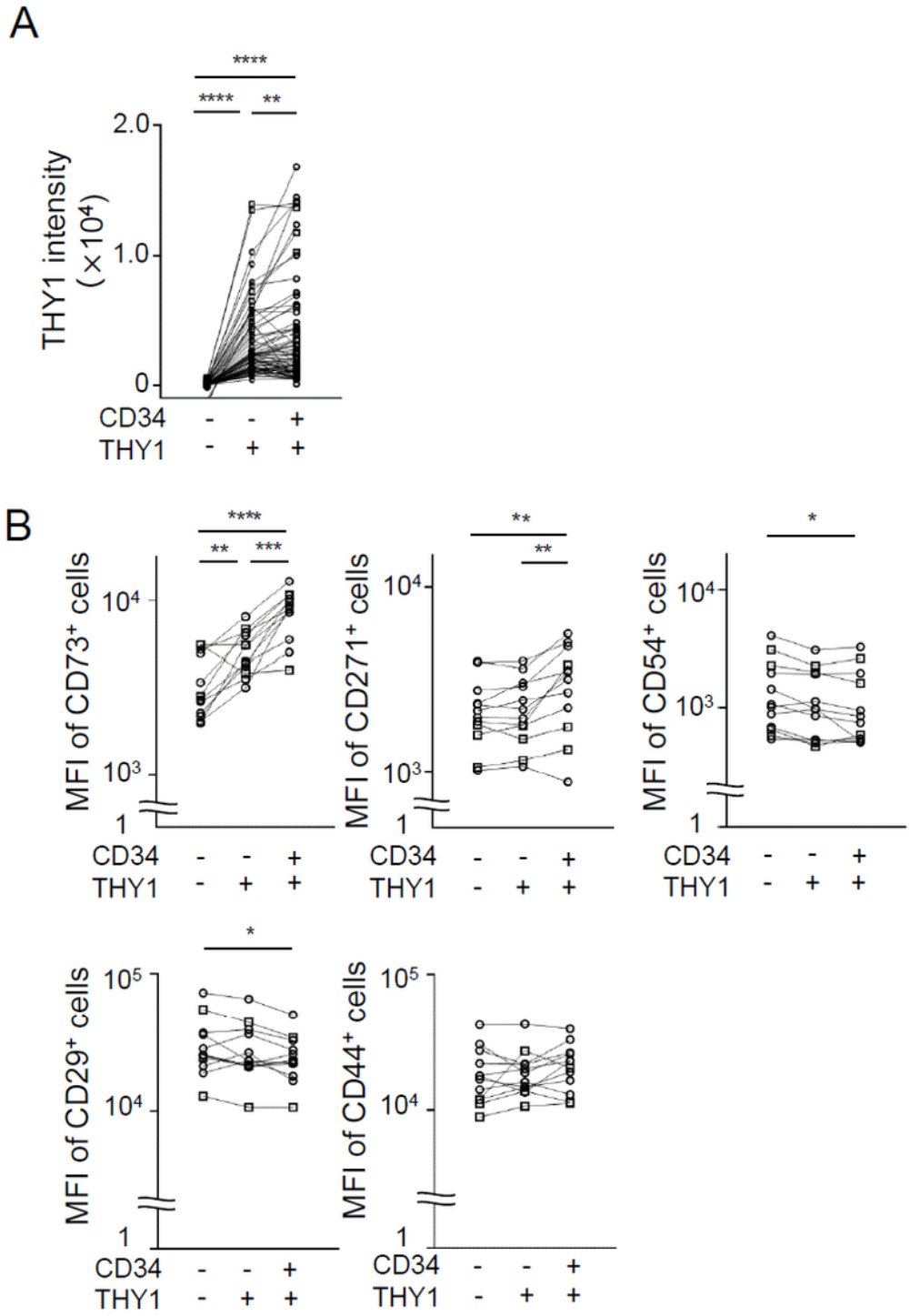

Figure 1

The expression of THY1 and MSC surface markers in the individual subset. A. THY1 expression. The mean fluorescence intensity (MFI) of THY1 was evaluated with flow cytometry. Data was shown in total samples OA+RA). B-D. MSC surface markers. The MFI of MSC surface markers (CD73, CD271, CD54, CD29 and CD44) was evaluated with flow cytometry. OA and RA samples are plotted as white circles and

white squares, respectively. Data were analyzed by Holm-Sidak's multiple comparison test for comparing each subset from the same samples (*p<0.05, **p<0.01, ***p<0.001, ****p<0.0001).

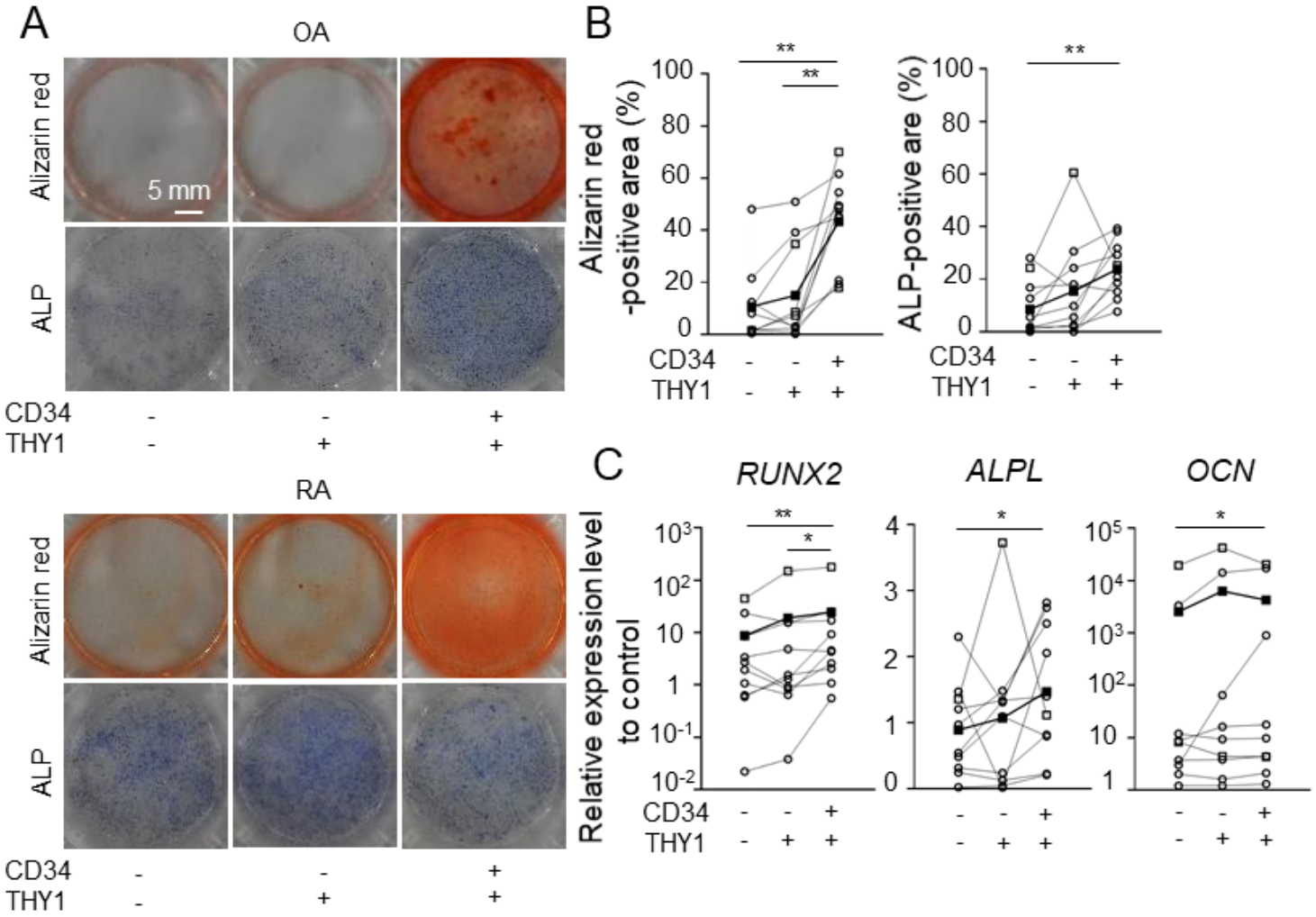

Figure 2

Osteogenic potentials of SF subsets. A. Representative photographs of whole dishes stained with alizarin red and ALP. Individual subsets were incubated in the calcification differentiation medium for 3 weeks. B. Quantification of the staining. Cells per donor were cultured in 3 dishes and the results of 10 donors for alizarin red and 11 donors for ALP were plotted. C. Gene expression levels by qPCR. The expression levels of the genes were plotted as a ratio to the expression level of 18S of undifferentiated SF as a control. Cells per donor were cultured in 3 dishes and the results of 10 donors for RUNX2 and ALPL, and 9 donors for OCN. OA and RA samples are plotted as white circles and white squares, respectively. The average data of each subset are plotted as black squares. Data were analyzed by Dunn's multiple comparison test for comparing each subset from the same patients (*p<0.05, **p<0.01).

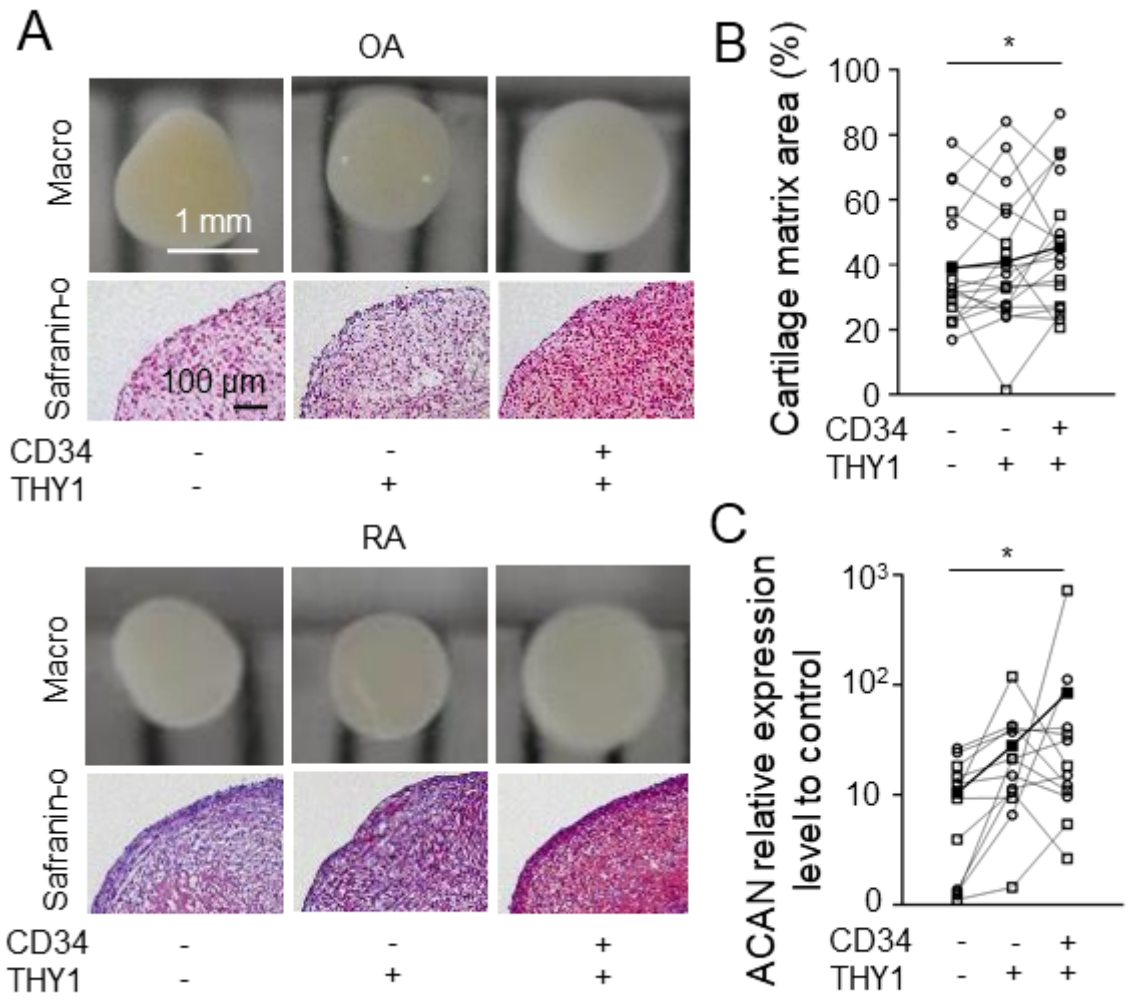

Figure 3

Chondrogenic potentials of SF subsets. A-B. Size and histology of the chondrocyte pellets. Individual subsets were incubated in the chondrocyte differentiation medium for 3 weeks. Representative macro picture of chondrocyte pellet (A, upper). Chondrocyte matrix was stained as red by safranin O staining and measured the ratio of stained area (A, lower B). Cells per donor were cultured in 3 pellets and the results of 18 donors (C). C. qPCR of chondrogenic differentiation marker. The relative expression levels of ACAN in differentiated cells. Cells per donor were cultured in 3 pellets and the results of 12 donors. The target genes were normalized with 18S of undifferentiated SF as a control. OA and RA samples are plotted as white circles and white squares, respectively. The average data of each subset are plotted as black squares. Data were analyzed by Dunn's multiple comparison test for comparing each subset from the same samples (*$p<0.05$).

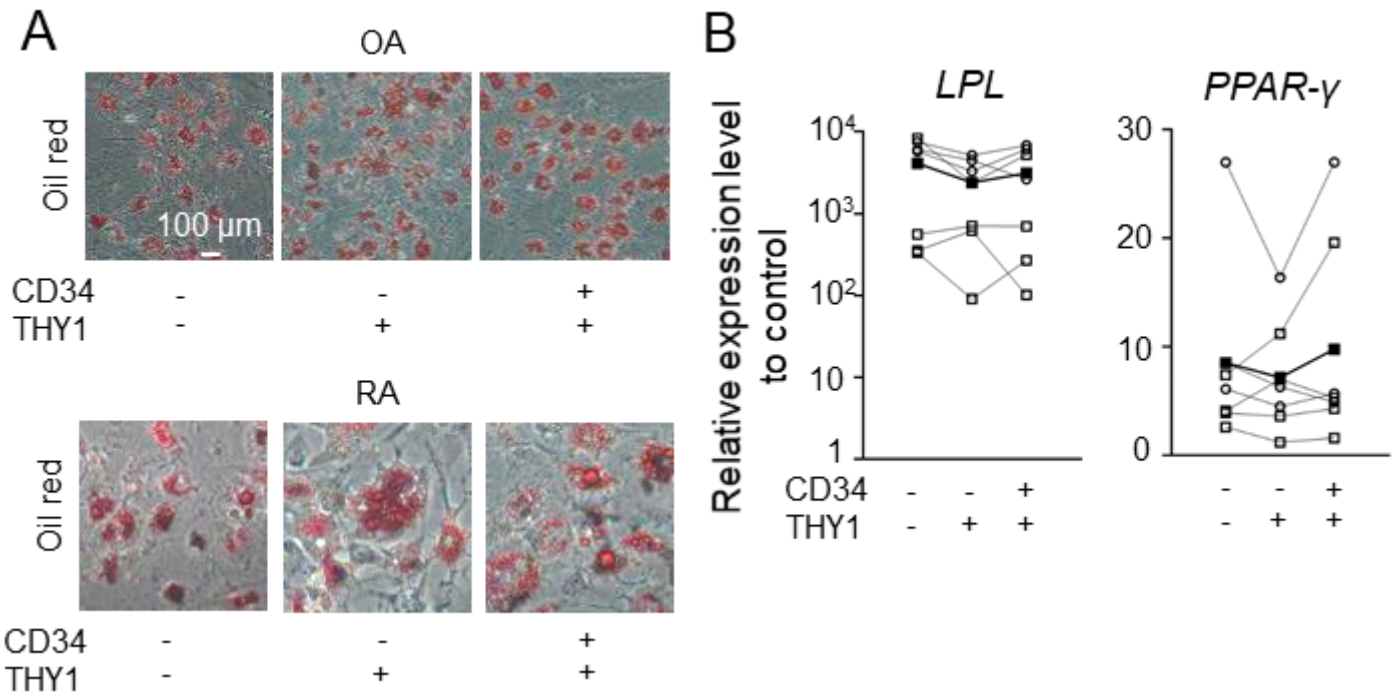

Figure 4

Adipogenic potential of SF subsets. A. Oil-red staining. The SF subsets cultured in adipocyte differentiation medium for 3 weeks. Adipogenesis was detected as red spots with oil-red staining. B. qPCR of adipogenic differentiation markers. The relative expression levels of LPL and PPARγ in differentiated cells. Cells per donor were cultured in 3 dishes and the results of 7 donors The target genes were normalized with 18S of undifferentiated SF as a control. OA and RA samples are plotted as white circles and white squares, respectively. The average data of each subset are plotted as black squares. Data were analyzed by Dunn's multiple comparison test for comparing each subset from the same samples.

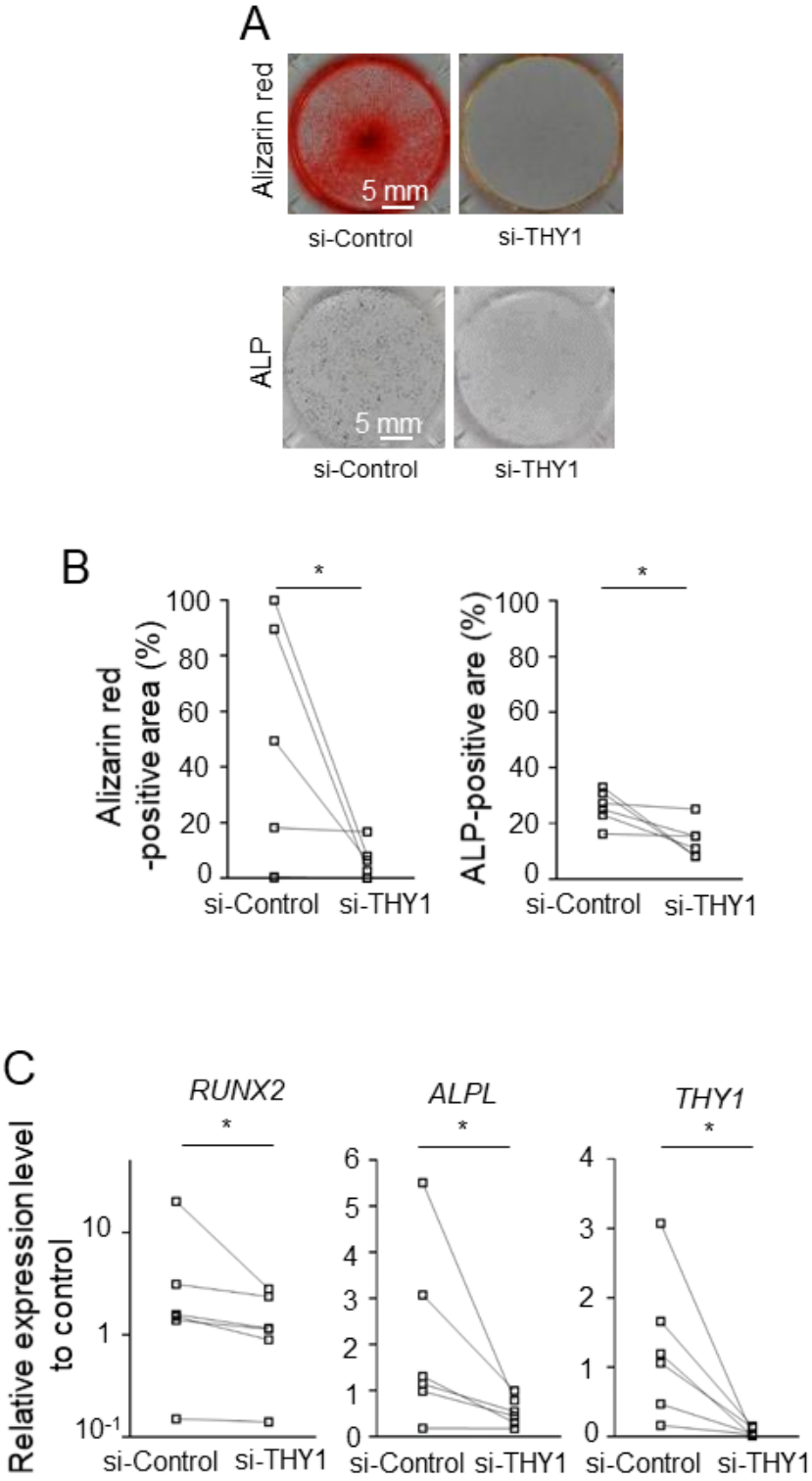

Figure 5

THY1 knockdown regulated osteoblast differentiation. A. Alizarin red and ALP staining. Representative pictures of SFs stained by alizarin red and ALP staining after THY1 knockdown. B. Quantification of staining. C. qPCR of osteogenic differentiation markers. Comparison of osteoblast differentiation markers at day 7 after THY1 knockdown. Cells per donor were cultured in 2 dishes and the results of 6

donors. The target genes were normalized with 18S of undifferentiated SF as a control. Data were analyzed by Wilcoxon's test for comparing each subset from the same samples (*p<0.05).

Supplementary Files

This is a list of supplementary files associated with this preprint. Click to download.

- SupplementaryFigure1.pdf
- SupplementaryFigure2.pdf
- SupplementaryFigure3.pdf